Efficient Visible Light Active CaFe2O4/WO3 Based Composite Photocatalysts: Effect of Interfacial Modification

3 AUTHORS, INCLUDING:

Zhifu Liu
Chinese Academy of Sciences
53 PUBLICATIONS **1,350** CITATIONS

SEE PROFILE

Masahiro Miyauchi
Tokyo Institute of Technology
96 PUBLICATIONS **3,471** CITATIONS

SEE PROFILE

Efficient Visible Light Active CaFe$_2$O$_4$/WO$_3$ Based Composite Photocatalysts: Effect of Interfacial Modification

Zhifu Liu, Zhi-Gang Zhao, and Masahiro Miyauchi*

Nanotechnology Research Institute, National Institute of Advanced Industrial Science and Technology, Central 5, 1-1-1 Higashi, Tsukuba, Ibaraki 305-8565, Japan

Received: July 1, 2009; Revised Manuscript Received: August 19, 2009

We report on the photocatalytic decomposition of acetaldehyde over CaFe$_2$O$_4$ (CFO)/WO$_3$ based composite photocatalysts under visible light irradiation, emphasizing the photocatalyst composition optimization and the effect of interface modification on photocatalytic activity. Although heat treatment caused deactivation of CFO/WO$_3$ composite photocatalyst, the photocatalytic activity of WO$_3$ was improved by simply mixing with CFO, and 5 wt % CFO coupled WO$_3$ showed the optimized performance. Ag and ITO coating on the CFO particle surface obviously promoted the photocatalytic activity of the CFO/WO$_3$ composite. The CFO/Ag (or ITO)/WO$_3$ composite photocatalyst could completely decompose acetaldehyde under visible light irradiation. X-ray photoelectron spectra suggested that the photoinduced self-reduction in WO$_3$ was effectively suppressed after coupling with CFO. The possible mechanism of the surface modification effects was discussed.

1. Introduction

Photocatalytic degradation of organic pollutants is one of the promising processes for environmental purification.[1,2] Great efforts were made to develop efficient visible light active photocatalysts to utilize the visible light that accounts for the largest proportion of the solar spectrum and artificial light sources. Since few materials can provide both photo-oxidation power and photoreduction power (which are necessary for complete decomposition of harmful organics) and, at the same time, can absorb visible light efficiently, composite photocatalysts with two or more components were extensively explored, and improved photocatalytic performance was obtained from various composite photocatalysts such as WO$_3$/TiO$_2$,[3] CdS/TiO$_2$,[4] Cu$_2$O/TiO$_2$,[5] WS$_2$/WO$_3$,[6,7] Co$_2$O$_3$/BiVO$_4$,[8] WO$_3$/SrNb$_2$O$_6$,[9] SnO$_2$/SrNb$_2$O$_6$,[10] Bi$_2$O$_3$/BaTiO$_3$,[11] CaFe$_2$O$_4$/PbBi$_2$Nb$_{0.9}$W$_{0.1}$O$_9$,[12] CdS/Au/TiO$_2$,[13] and WO$_3$/W/PbBi$_2$Nb$_{1.9}$Ti$_{0.1}$O$_9$.[14] Several approaches were reported for composite photocatalysts design. The general concept is that the combined semiconductors should have different band gaps so that charge separation can be enhanced by the internal electric field driving force. Nozik developed the photochemical diode concept by combining a p-type and an n-type semiconductor.[15] Efficient composite photocatalyst was also obtained on the basis of the Z-scheme mechanism.[13] For the composite photocatalysts, a chemically bonded interface between the semiconductors is normally preferred for efficient charge separation.[7–11] So many works have been carried out to get good junctions by mechanical alloying, in situ synthesis, physical or chemical vapor deposition, etc.[7–11,16] Recently, Sayama et al.[17–19] reported the efficient visible light photocatalysts by just mixing the p-type CuO or CuBi$_2$O$_4$ powder with WO$_3$. Although efficient charge transfer may not happen at the interface of the two components in the mechanically mixed system, the interfaces should be very important because they are the only pass connecting the different components. The high activity of both chemically bonded and simply mixed composite photocatalysts stimulates us to investigate the effects of interface modification on the photocatalytic activity of a composite photocatalyst.

Tungsten oxide (WO$_3$) is an n-type semiconductor with the optical absorption edge locating in the visible range ($E_g = 2.5-2.8$ eV).[20] The strong oxidizing power of the photogenerated holes in WO$_3$ makes it an attractive candidate of visible light responsive photocatalyst for photooxidation of organic pollutants. However, the reduction potential of photogenerated electrons in the conduction band of WO$_3$ ranges from +0.3 V to +0.5 V versus NHE,[21] which is much more positive than the one-electron reduction potential of adsorbed oxygen (e$^-$ + O$_2$(s) + H$^+$ → HO$_2$$^\bullet$, $E = -0.046$ V vs NHE).[22] As a result, it is difficult for the photogenerated electrons in WO$_3$ to activate oxygen molecules through the one-electron reduction process. This was thought to be the main reason of the low activity of pure WO$_3$ photocatalyst.[23] However, the strong oxidation power and the leak of reduction power make WO$_3$ an idea model material for exploring new composite photocatalysts and for monitoring the electron behavior in a composite photocatalyst.

We have reported the superhydrophilic conversion of the CaFe$_2$O$_4$(CFO)/ITO/WO$_3$ multilayer thin film, which showed highly enhanced performance compared with pure WO$_3$ film.[24] In this paper, we focused on the photocatalytic performance of the CFO/WO$_3$ powder photocatalysts. The photocatalytic activity of WO$_3$ was largely improved by coupling with CFO, and the composite photocatalysts can decompose acetaldehyde completely. The effects of interface modification using metallic layers on the photocatalytic performance were investigated.

2. Experimental Section

The CFO fine powders were synthesized by a solution method. Calcium acetate monohydrate and iron(III) nitrate enneahydrate (Wako Pure Chemical Industries, Ltd.) were used as precursors. In a typical experiment, 0.88 g of calcium acetate monohydrate and 4.04 g of iron nitrate enneahydrate were dissolved in 25 mL of deionized water. Then, 5 mL of polyethylene glycol (PEG) (molecular weight of about 3500 kg/mol) aqueous solution (5 wt %) was added to the above solution.

CaFe$_2$O$_4$/WO$_3$ Based Composite Photocatalysts

J. Phys. Chem. C, Vol. 113, No. 39, 2009 **17133**

A kind of gray dry gel-like powder remained after evaporating the solvent under stirring at 120 °C. Finally, CFO fine powder was obtained by calcining the dry gel at 450 °C for 2 h and 1050 °C for 10 h. WO$_3$ powders were purchased from the High Purity Chemicals Institute, Inc. For preparing the photocatalysts, a proper amount of CFO was mixed with 0.5 g of WO$_3$ powder in a quartz mortar with full hand force in the presence of a small amount of deionized water. The mixture was ready for characterizations after being dried in an oven at 60 °C overnight. To investigate the surface modification effect, some samples were treated at 400 °C for 1 h in air.

The surfaces of CFO and WO$_3$ were also modified with Ag or ITO. Ag fine particles were deposited on either CFO or WO$_3$ powders by the photoreduction method before they were mixed. In detail, a proper amount of CFO or WO$_3$ powders was dispersed in 5 mL of 0.01 M AgNO$_3$ aqueous solution. Several drops of ethanol were added into the mixture. Then, the mixture was irradiated under 5 mW/cm^2 UV light for 30 min under stirring. Finally, the powders were separated by centrifuge and washed with deionized water four times. For ITO coating, the CFO or WO$_3$ powders were immersed into ITO solution (containing 0.18 M In(NO$_3$)$_3$ and 0.01 M SnCl$_4$) for 10 min. Then, the powders were separated by filtration. The modified powders were dried at 60 °C overnight before use.

X-ray diffraction (XRD) characterization was performed on a Rigaku Rint 2500 VH/PC X-ray diffractometer. The morphology of the materials was observed on a field emission scanning electron microscope (FE-SEM) (HITACHI S-4800). The absorption spectra of the photocatalysts were measured on an UV−visible spectrophotometer (JASCO V-660) with an integration sphere using a reflection mode. X-ray photoelectron spectroscopy (XPS) analysis was carried out on a Quantum 2000 scanning ESCA microprobe system (Physical Electronics, Inc.).

A typical VOC pollutant, acetaldehyde, was used as the probe molecule for evaluating the photocatalytic activity. For the photocatalytic measurements, 0.1 g of photocatalyst was uniformly dispersed on a circular glass dish, which was then mounted in a cylindrical glass static reactor (0.5 L in volume) with a quartz window. The O$_2$ (20%)−N$_2$ mixture adjusted to a relative humidity of 50% was used to fill the reaction vessel. Acetaldehyde vapor was introduced into the reactor by syringe until the concentration reached about 500 ppm. The sample was illuminated with a 150 W Xe lamp light source (Hayashi LA-410UV) under an intensity of 80 mW/cm^2. Optical filters of Y-43 and C-50S (Asahi Technoglass) were used to cut off the ultraviolet and infrared radiation. The concentrations of acetaldehyde and generated CO$_2$ were measured using a gas chromatograph (Shimadzu, GC-8A) equipped with a 2 m Porapak-Q column, a flame ionization detector, and a methanizer.

3. Results and Discussion

3.1. Characterization of CFO. CFO has an orthorhombic structure and normally exhibits a p-type semiconducting property.[25,26] There were reports on the photoreduction of water and CO$_2$ using CFO for its high conduction band level (−0.4 eV, NHE) and therefore strong reduction power.[26−28] Because of its cheap and wide availability, CFO is also used as a pigment material.[29] In this work, we studied the photocatalytic properties of CFO coupled WO$_3$ composites. CFO fine powders were synthesized using a solution based method. The XRD pattern of the synthesized CFO powder as shown in Figure 1 can match well with the documented XRD data of CaFe$_2$O$_4$ (JCPDS card No. 32-0168), which indicated that well crystallized single phase
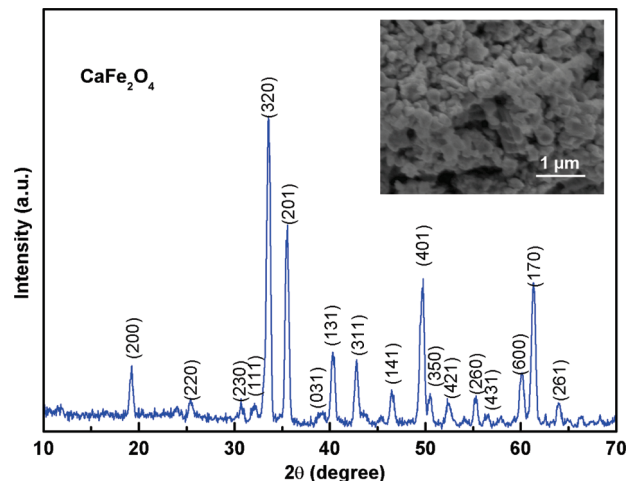

Figure 1. XRD pattern of the synthesized CFO powder. The inset is the SEM image of the corresponding sample.
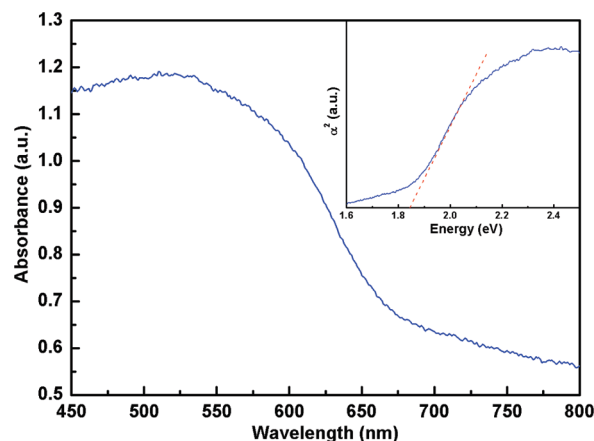

Figure 2. Absorption spectrum of CFO powder. The inset shows the square of the coefficient as a function of photon energy.

CFO has been obtained. The SEM image inset in Figure 1 shows that the CFO powders have a diameter in the range 100−300 nm.

The CFO powders have deep brown color and show strong absorption of visible light. The absorption spectrum of the CFO powder is presented in Figure 2, which shows an obvious absorption edge at about 670 nm. This absorption should correspond to the direct band absorption of CFO. The band gap was evaluated to be about 1.85 eV according to the energy dependence relation of $\alpha^2(h\nu) \propto (h\nu - E_g)$, where α and E_g are the absorption coefficient and the energy gap of a semiconductor. This band gap value is compatible with that of the reported bulk CFO.[26] The narrow band gap allows CFO to absorb a wide range of visible light.

3.2. CFO/WO$_3$ Composite. The CFO coupled WO$_3$ composite was obtained by mechanically mixing the two powders with different ratios. The absorption spectra of the pure WO$_3$ and CFO/WO$_3$ composites are presented in Figure 3. Pure WO$_3$ has an obvious absorption edge at about 450 nm corresponding to the WO$_3$ band transition. Tail absorption at 600−800 nm should be caused by the existence of W^{5+}, which is also the reason why the pure WO$_3$ shows yellow-green color.[30] The CFO/WO$_3$ composites have gray color, and the absorption spectra show obvious superposition of the absorption of WO$_3$ and CFO. The absorption of CFO increases with the increase of CFO ratio in the composite. The absorption band of WO$_3$ at about 450 nm has no obvious change. However, we notice that the
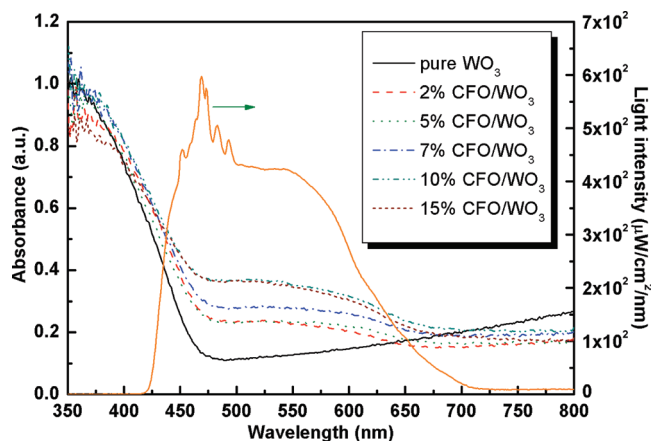
Figure 3. Absorption spectra of pure WO_3 and CFO/WO_3 composites with 2, 5, 7, 10, and 15 wt % CFO. The spectrum of light source for photocatalytic reaction is also shown.
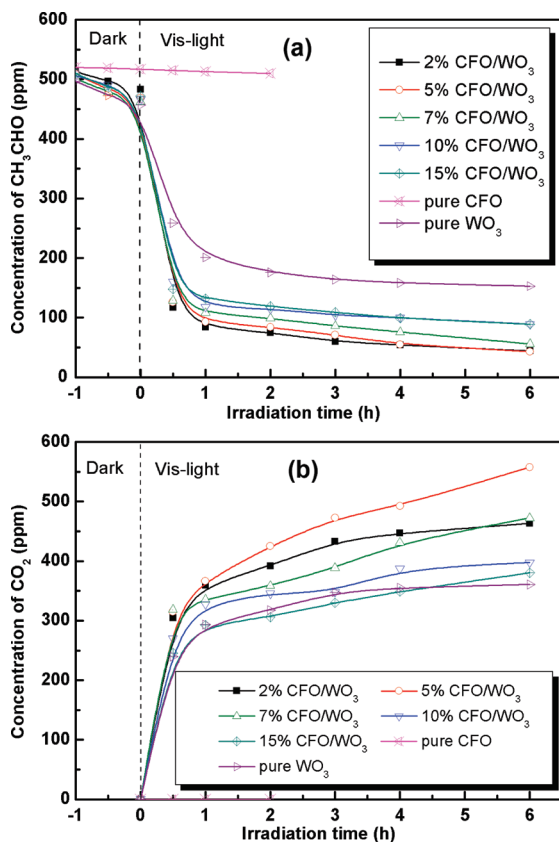

Figure 4. Time dependent profile of acetaldehyde decomposition and CO_2 generation over CFO/WO_3 composite photocatalysts under visible light irradiation (80 mW/cm²). The results over pure WO_3 and CFO are also plotted for comparison.

absorption tail of WO_3 is suppressed to some extent for the CFO/WO_3 composite, indicating the decrease of the W^{5+} amount in the composite. The spectrum of the light source for photocatalytic reaction is also shown in Figure 3, which indicates that both WO_3 and CFO can absorb the light.

The photocatalytic activity of the CFO/WO_3 composites was evaluated by decomposing acetaldehyde under visible light irradiation (>420 nm). Figure 4 depicts the acetaldehyde decomposing and CO_2 generation profile over different photocatalysts as a function of visible light irradiation time. No CO_2 can be generated over pure CFO. The amount of acetaldehyde has also no change over CFO even after a long time irradiation,

indicating that CFO itself shows no photocatalytic activity for decomposing acetaldehyde. However, CFO coupling can obviously improve the activity of WO_3. WO_3 coupled with 5 wt % CFO shows the highest photocatalytic activity for decomposing acetaldehyde to CO_2. Under this condition, the ratio of absorbed photon numbers between CFO and WO_3 is 2:1, which can be calculated from the absorption spectra shown in Figure 3. Further increase in the CFO amount leads to the decrease of the photocatalytic activity of the CFO/WO_3 composite. The CO_2 generation almost stops over pure WO_3 photocatalyst after irradiation of more than 4 h.

The presented experiments were carried out under light-limited conditions.[31] The photocatalytic activity strongly depends on the electron−hole separation efficiency of the photocatalyst. The photodecomposition of acetaldehyde on TiO_2 has been reported to follow a radical-chain mechanism.[32,33] Although photogenerated holes can directly oxidize organic molecules, the activation of oxygen by the photogenerated electrons is very important for complete oxidation of organics to CO_2 and H_2O.[31] However, it is difficult for the one-electron oxygen activation process to happen on pure WO_3 because of its low conduction band level (more positive to vacuum). Instead, the following reactions more easily occur:[34,35]

$$WO_3 + e^- + H^+ \rightarrow H_xWO_3 \quad \text{or} \quad WO_3 + e^- + H^+ \rightarrow WO_{3-\delta} + H_2O$$
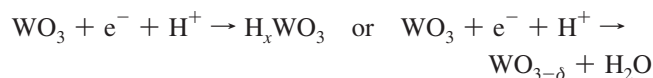
Part of the photogenerated electrons can be trapped by WO_3 itself through the above reaction, which leads to charge separation. This may be one of the reasons that the pure WO_3 shows high initial photocatalytic activity. Since the electron capacity of WO_3 is limited. The electrons may accumulate on the surface of WO_3 and the possibility of electron−hole recombination increases after some time. As a result, the photodecomposition reaction slows down. The absence of active oxygen results in the production of intermediate compounds like acetic acid over pure WO_3 catalyst,[17] and the CO_2 generation stops only after several hours of irradiation. The coupling of CFO with WO_3 may consume some electrons accumulating on WO_3 and contribute to the steady generation of CO_2 after the initial high-speed reaction.

To clarify the origin of the photocatalytic activity increase in CFO/WO_3 composite photocatalyst, we investigated the chemical state of photocatalysts before and after the photocatalytic reaction using XPS. Figure 5 represents the XPS spectra of W4f, O1s, Ca2p, and Fe2p of pure WO_3 and the CFO/WO_3 composite photocatalysts. For pure WO_3, the W4f peaks of the XPS spectra are obviously broadened after the photocatalytic reaction. This kind of broadening is caused by the partial transition of W^{6+} to W^{5+}.[36] On the other hand, for CFO/WO_3 composite photocatalyst, no obvious change can be found from XPS spectra of the W, Ca, and Fe elements of the CFO/WO_3 composite photocatalyst before and after the photocatalytic reaction. The results imply that the self-reduction process by photogenerated electrons in WO_3 was hinted after coupling with CFO.

The improved photocatalytic performance of the composite photocatalyst was mostly explained by the enhanced charge separation,[7−13,18,30−32] or the multielectron process.[37−40] Irie et al. reported that improved visible light activity in Cu^{2+} modified WO_3.[40] They indicated the formation of Cu^{1+} under visible light irradiation, and these Cu^{2+}/Cu^{1+} redox couples are essential to cause multielectron reduction of oxygen molecules.[39] In the

CaFe$_2$O$_4$/WO$_3$ Based Composite Photocatalysts

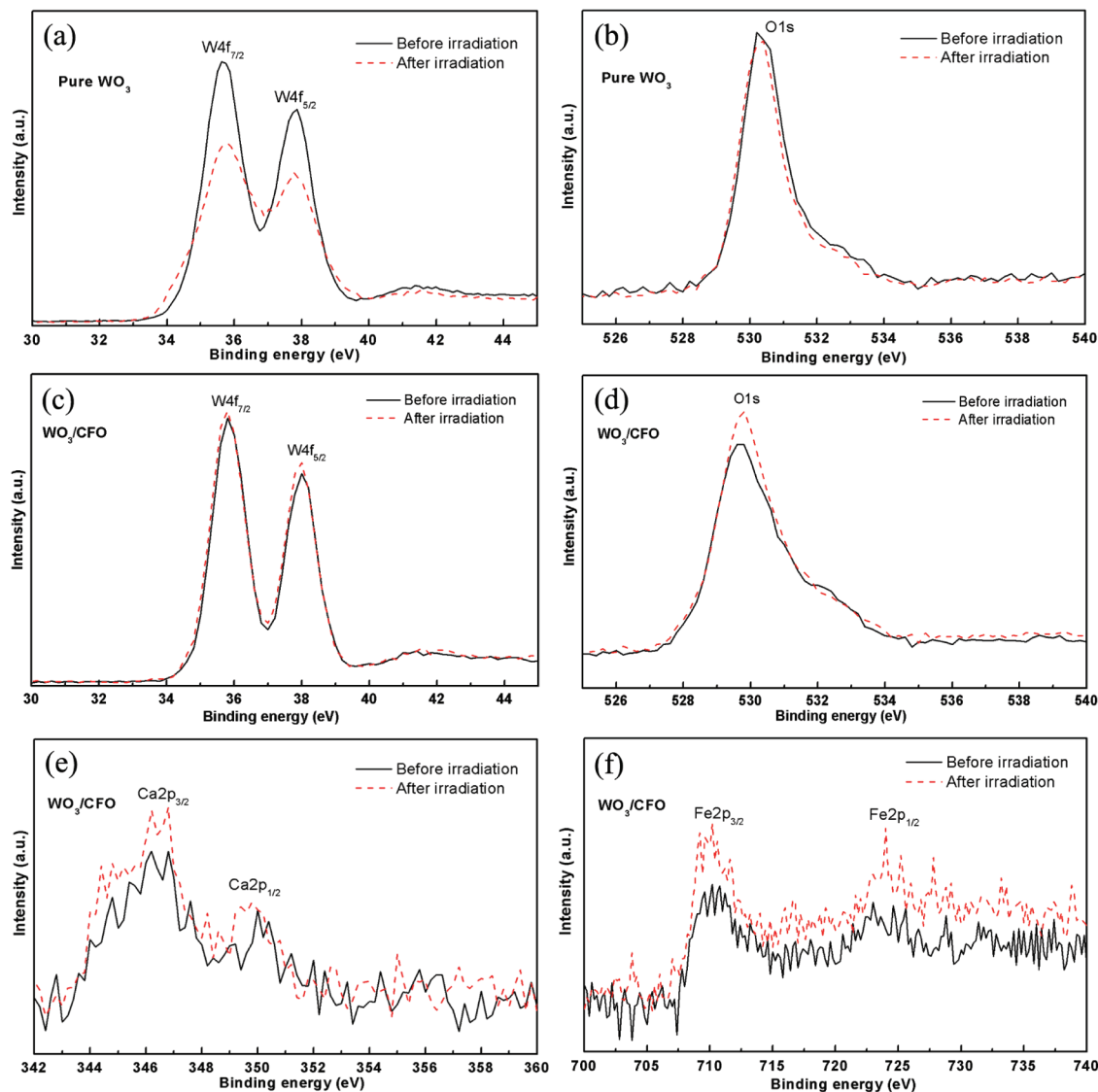*J. Phys. Chem. C, Vol. 113, No. 39, 2009* **17135**

Figure 5. XPS spectra of the photocatalysts before and after photocatalysis reactions: (a) pure WO$_3$; (b–d) 5% CFO/WO$_3$ composite.

present work, our XPS data revealed that both the Ca^{2+} and Fe^{3+} are stable under light irradiation, indicating that the CFO does not act as a cocatalyst like the Cu^{2+}. In the CFO/WO$_3$ system, CFO has a much higher (more negative) conduction band level than WO$_3$. There is a high barrier for electrons to transfer from the conduction band of WO$_3$ to that of CFO. In addition, neither WO$_3$ nor CFO can store the electrons like the Cu^{2+} or noble metal materials to let the multielectron process happen. Considering the p-type character of CFO, one possible way is that the photogenerated electrons in WO$_3$ recombine with photogenerated holes in CFO at the interface like what happens in a photoelectrochemical diode.[14,15]

The enhanced photocatalytic activity based on the p–n semiconductor system has been reported by several groups, all of which tried to make a good junction between the materials.[8,12,41,42] Ohmic contacting at the interface of the p-type and n-type materials is preferred to enhance the charge separation.[14,15] In this work, it was found that the photocatalytic activity of WO$_3$ could be improved by just simply mixing with CFO. Obviously, a good junction cannot be formed in the mixed powder system. Sayama et al. suggested that the defects at the interface of composite photocatalyst play important roles in the photocatalytic reactions.[18] In fact, some interfacial states which are formed by dangling bonds, interatomic spaces, surface

hydroxyl groups, etc., should exist between the particles.[43] The interfacial states between CFO and WO$_3$ can be traps of both electrons and holes. To investigate the effect of interface on the photocatalytic properties, we did a modification on the surface of WO$_3$ and CFO particles.

3.3. Surface Modification. Since the surface defects are very sensitive to heat treatment, we treated the CFO/WO$_3$ composite at 400 °C for 1 h. Ag and ITO were also coated on the WO$_3$ or CFO particle surface before they were mixed. Figure 6 shows the photogenerated CO$_2$ concentration as a function of light irradiation time over the CFO/WO$_3$ composite photocatalysts with different surface modification. We can see that, when we deposited Ag or ITO on the pure WO$_3$ surface, the modified WO$_3$ (Ag@WO$_3$, ITO@WO$_3$) did not show improved activity during the 6 h of irradiation. Actually, the initial activity of modified WO$_3$ is much lower than that of pure WO$_3$. The photocatalytic activity of the CFO/WO$_3$ composite largely decreases after heat treatment at 400 °C for 1 h. The CO$_2$ generation speed is much higher over composite photocatalysts composing of Ag or ITO coated CFO (Ag@CFO/WO$_3$, ITO@CFO/WO$_3$) than over CFO/WO$_3$ photocatalyst. If the Ag or ITO coating was coated on WO$_3$ particles, the overall activity of the composites (CFO/Ag@WO$_3$, CFO/ITO@WO$_3$) is also improved compared with that of CFO/WO$_3$, although the initial
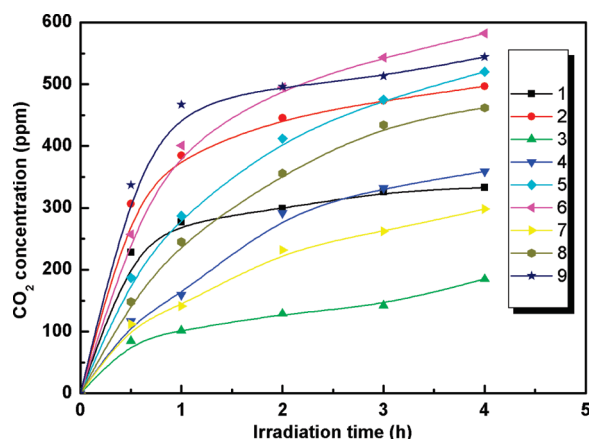
Figure 6. Photogenerated CO_2 over different photocatalysts under visible light as a function of irradiation time: (1) pure WO_3; (2) CFO/WO_3; (3) heat treated CFO/WO_3; (4) Ag@WO_3; (5) CFO/Ag@WO_3; (6) Ag@CFO/WO_3; (7) ITO@WO_3; (8) CFO/ITO@WO_3; (9) ITO@CFO/ WO_3. 5 wt % CFO was used in the composite photocatalysts. The initial acetaldehyde concentration is 500 ppm. The visible light density is 80 mW/cm^2.
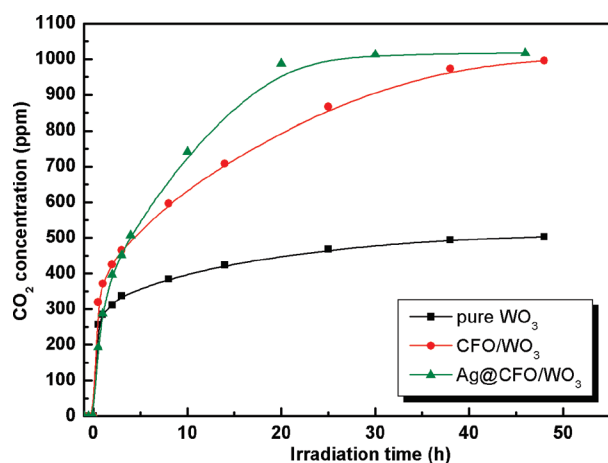

Figure 7. CO_2 photogeneration profile at a long time visible irradiation. The initial acetaldehyde concentration is 500 ppm. The visible light density is 80 mW/cm^2.

activity is decreased. These results indicate that modifying the interface of CFO/WO_3 composite with a metallic layer can improve the photocatalytic activity.

We also compared the ability of completely decomposing acetaldehyde over these composite photocatalysts. The acetaldehyde can be completely decomposed to CO_2 over all of the CFO/WO_3 based composite photocatalysts (decomposing 500 ppm acetaldehyde to 1000 ppm CO_2) at prolonged irradiation time. Figure 7 presents the CO_2 generation profile over pure

WO_3, 5 wt % CFO/WO_3, Ag@CFO/WO_3 photocatalysts. The CO_2 generation almost stops after 40 h of irradiation over pure WO_3. Pure WO_3 cannot completely decompose acetaldehyde to CO_2 over even more than 100 h under the present experimental conditions. However, the acetaldehyde can be completely decomposed to CO_2 over 5 wt % CFO/WO_3 composite in 48 h. It is impressive that the Ag modified composite Ag@CFO/WO_3 can reach complete decomposition of acetaldehyde in 20 h, which is more than 2 times faster than the CFO/WO_3 photocatalysts.

The experimental results indicate that the interfaces among the particles of the CFO/WO_3 composite play an important role in the photocatalytic reaction. In this work, the heat treatment temperature is only 400 °C and is not high enough to cause chemical reaction between CFO and WO_3. We believe that heat treatment reduced the defect states such as dangling bonds and surface hydroxyl groups at the surface of the particles. Figure 8 shows the schematic diagrams of the energy levels of the composites under different conditions. The perfect p−n junction structure between two semiconductors shown in Figure 8a is impossible to be achieved by simply mixing two components. In addition, holes or electrons in the perfect p−n junction structure do not have enough oxidative or reductive potential for complete oxidation of organics. For the just mixed CFO/ WO_3 composite, there may be intermediate levels at the interface formed by defect states, which could act as traps of photogenerated holes or electrons and enhance the charge separation in both n-type WO_3 and p-type CFO (Figure 8b). The decrease of the activity of the heat treated sample implies that the defect states at the interface play important roles in the photocatalytic reaction. Modifying the particle surface using metallic Ag and ITO makes the CFO−WO_3 connection more like ohmic contacting p−n junction. As shown in Figure 8c, photogenerated holes in p-type CFO and electrons in n-type WO_3 recombine at the metallic contacting position and promote the charge separation, as a result, increasing the photocatalytic activity. Previous reports indicated that a chemically bonded interface can enhance the charge separation driven by the internal electric field.[6,10−12] In the present work, interfacial modification using a metallic layer also enhanced the charge separation, while the driving force for the charge separation in the ohmic contacting p−n junction is the band bending at the interface, which keeps the photogenerated electrons at the higher conduction band and the photogenerated holes in the lower valence band so that both the strong oxidation power of the n-type semiconductor and strong reduction power of the p-type semiconductor can be utilized. This is preferred for the complete decomposition of harmful organics in gas phase reactions. The relatively lower initial activity of the photocatalysts containing a metallic layer coated WO_3 particle may be caused by the blocking effect of the surface layer.
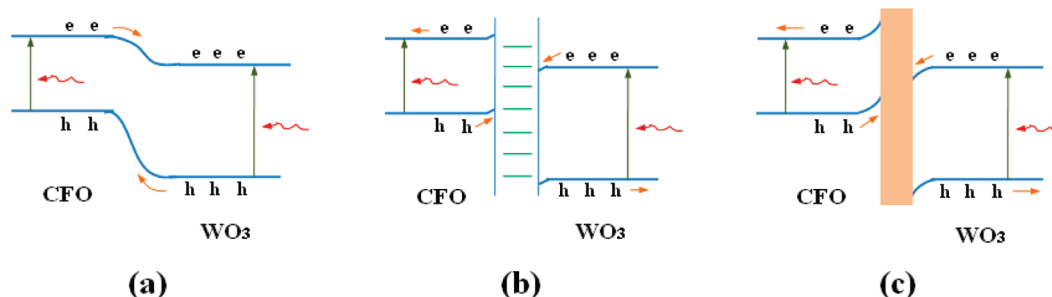

Figure 8. Schematic diagrams of the energy levels of the CFO/WO_3 composite: (a) perfect junction; (b) with defect levels at interface; (c) ohmic contact junction.

CaFe₂O₄/WO₃ Based Composite Photocatalysts

J. Phys. Chem. C, Vol. 113, No. 39, 2009 **17137**

The CFO/WO₃ composite photocatalyst works by simultaneously absorbing two photons (one in each semiconductor). The light absorption efficiency, electron–hole pair generation ability, and carrier mobility in the materials have large effects on the photocatalytic properties. The matching of photogenerated electrons and holes between the two semiconductor materials are key factors to optimizing the performance of the junction photocatalysts. The optimum amount of CFO in CFO/WO₃ is 5 wt %, and the corresponding absorbed photon number in CFO to that in WO₃ was about 2:1. The much higher absorption coefficient of CFO in the visible region than that of WO₃ may be one reason for the low optimum ratio of 5% CFO in the CFO/WO₃ system. On the other hand, we investigated the photocatalytic properties in powder form in the present study, but the concept of interfacial modification should also be very valuable for designing thin film based photocatalysts for various applications such as air purification and self-cleaning.

4. Conclusions

Efficient visible light active CFO/WO₃ based composite photocatalysts were prepared, and the photocatalytic performance was investigated. The composite containing 5 wt % CFO showed optimized performance. Surface modification was made by heating the CFO/WO₃ composite or by coating the particle surface with Ag or ITO. The photocatalytic activity can be largely improved by coating the CFO particles with a Ag or ITO layer. The acetaldehyde decomposing speed is more than 2 times faster over Ag@CFO/WO₃ than over CFO/WO₃ photocatalyst. The photocatalytic activity enhancement is attributed to the efficient charge separation resulting from the recombination of the photogenerated charge carriers at the ohmic contact interface.

References and Notes

(1) Fujishima, A.; Hashimoto, K.; Watanabe, T. *TiO₂ photocatalysis: fundamentals and applications*; BKC, Inc.: Tokyo, 1999.
(2) Choi, W. *Catal. Surv. Asia* **2006**, *10*, 16.
(3) Papp, J.; Soled, S; Dwight, K.; Wold, A. *Chem. Mater.* **1994**, *6*, 496.
(4) Jang, J. S.; Li, W.; Oh, S. H.; Lee, J. S. *Chem. Phys. Lett.* **2006**, *425*, 278.
(5) Zhang, Y.; Ma, L.; Li, J.; Yu, Y. *Environ. Sci. Technol.* **2007**, *41*, 6264.
(6) Paola, A. D.; Palmisano, L.; Venezia, A. M.; Augugliaro, V. *J. Phys. Chem. B* **1999**, *103*, 8236.

(7) Paola, A. D.; Palmisano, L.; Augugliaro, V. *Catal. Today* **2000**, *58*, 141.
(8) Long, M.; Cai, W.; Cai, J.; Zhou, B.; Chai, X.; Wu, Y. *J. Phys. Chem. B* **2006**, *110*, 20211.
(9) Huang, H.; Lin, X.; Xing, J.; Wang, W.; Shan, Z.; Huang, F. *Mater. Sci. Eng., B* **2007**, *141*, 49.
(10) Lin, X.; Huang, F.; Xing, J.; Wang, W.; Xu, F. *Acta Mater.* **2008**, *56*, 2699.
(11) Lin, X.; Xing, J.; Wang, W.; Shan, Z.; Xu, F.; Huang, F. *J. Phys. Chem. C* **2007**, *111*, 18288.
(12) Kim, H. G.; Borse, P. H.; Choi, W.; Lee, J. S. *Angew. Chem., Int. Ed.* **2005**, *44*, 4585.
(13) Tada, H.; Mitsui, T.; Kiyonaga, T.; Akita, T.; Tanaka, K. *Nat. Mater.* **2006**, *5*, 782.
(14) Kim, H. G.; Jeong, E. D.; Borse, P. H.; Jeon, S.; Yong, K.; Lee, J. S.; Li, W.; Oh, S. H. *Appl. Phys. Lett.* **2006**, *89*, 064103.
(15) Nozik, A. J. *Appl. Phys. Lett.* **1977**, *30*, 567.
(16) Puddu, V.; Mokaya, R.; Puma, G. L. *Chem. Commun.* **2007**, 4749.
(17) Arai, T.; Yanagida, M.; Konishi, Y.; Iwasaki, Y.; Sugihara, H.; Sayama, K. *Catal. Commun.* **2008**, *9*, 1254.
(18) Arai, T.; Yanagida, M.; Konishi, Y.; Iwasaki, Y.; Sugihara, H.; Sayama, K. *J. Phys. Chem. C* **2007**, *111*, 7574.
(19) Arai, T.; Horiguchi, M.; Yanagida, M.; Gunji, T.; Sugihara, H.; Sayama, K. *J. Phys. Chem. C* **2009**, *113*, 6602.
(20) Kleperis, J.; Zubkans, J.; Lusis, A. R. *Proc. SPIE* **1997**, *2968*, 186.
(21) Bamwenda, G. R.; Arakawa, H. *Appl. Catal., A* **2001**, *210*, 181.
(22) Torimoto, T.; Nakamura, N.; Ikeda, S.; Ohtani, B. *Phys. Chem. Chem. Phys.* **2002**, *4*, 5910.
(23) Arai, T.; Yanagida, M.; Konishi, Y.; Ikura, A.; Iwasaki, Y.; Sugihara, H.; Sayama, K. *Appl. Catal., B* **2008**, *84*, 42.
(24) Liu, Z.; Miyauchi, M. *Chem. Commun.* **2009**, 2002.
(25) Baur, W. H. *J. Solid State Chem.* **1982**, *43*, 222.
(26) Matsumoto, Y.; Omae, M.; Sugiyama, K.; Sato, E. *J. Phys. Chem.* **1987**, *91*, 577.
(27) Matsumoto, Y. *J. Solid State Chem.* **1996**, *126*, 227.
(28) Matsumoto, Y.; Obata, M.; Hombo, J. *J. Phys. Chem.* **1994**, *98*, 2950.
(29) Candeia, R.; Bernardi, M.; Longo, E.; Santos, I.; Souza, A. *Mater. Lett.* **2004**, *58*, 569.
(30) Fujii, M.; Kawai, T.; Nakamatsu, T.; Kawai, S. *J. Chem. Soc., Chem. Commun.* **1983**, 1428.
(31) Ohko, Y.; Hashimoto, K.; Fujishima, A. *J. Phys. Chem. A* **1997**, *101*, 8057.
(32) Pelizzetti, Z.; Minero, C. *Electrochim. Acta* **1993**, *38*, 47.
(33) Ohko, Y.; Tryk, D. A.; Hashimoto, K.; Fujishima, A. *J. Phys. Chem. B* **1998**, *102*, 2699.
(34) Bechinger, C.; Oefinger, G.; Herminghaus, S.; Leiderer, P. *J. Appl. Phys.* **1993**, *74*, 4527.
(35) Chang, I. F.; Gilbert, B. L.; Sun, T. I. *J. Electrochem. Soc.* **1975**, *122*, 955.
(36) Romanyuk, A.; Oelhafen, P. *Sol. Energy Mater. Sol. Cells* **2006**, *90*, 1945.
(37) Abe, R.; Takami, H.; Murakami, N.; Ohtani, B. *J. Am. Chem. Soc.* **2008**, *130*, 7780.
(38) Kim, Y.; Irie, H.; Hashimoto, K. *Appl. Phys. Lett.* **2008**, *92*, 182107.
(39) Irie, H.; Kamiya, K.; Shibanuma, T.; Miura, S.; Tryk, D. A.; Yokoyama, T.; Hashimoto, K. *J. Phys. Chem. C* **2009**, *113*, 10761.
(40) Irie, H.; Miura, S.; Kamiya, K.; Hashimoto, K. *Chem. Phys. Lett.* **2008**, *457*, 202.
(41) Ye, F.; Ohmori, A.; Li, C. *J. Mater. Sci.* **2004**, *39*, 353.
(42) Chen, Y.; Crittenden, J. C.; Hackney, S.; Sutter, L.; Hand, W. D. *Environ. Sci. Technol.* **2005**, *39*, 1201.
(43) Sah, C.-T. *Fundamentals of Solid-State Electronics*; World Sci. Pub. Co Inc: Singapore, 1991.